Hindawi Publishing Corporation
Mathematical Problems in Engineering
Volume 2007, Article ID 62157, 17 pages
doi:10.1155/2007/62157

Research Article

Dynamic Stationary Response of Reinforced Plates by the Boundary Element Method

Luiz Carlos Facundo Sanches, Euclides Mesquita, Renato Pavanello, and Leandro Palermo Jr.

Received 1 October 2006; Revised 7 February 2007; Accepted 26 February 2007

Recommended by José Manoel Balthazar

A direct version of the boundary element method (BEM) is developed to model the stationary dynamic response of reinforced plate structures, such as reinforced panels in buildings, automobiles, and airplanes. The dynamic stationary fundamental solutions of thin plates and plane stress state are used to transform the governing partial differential equations into boundary integral equations (BIEs). Two sets of uncoupled BIEs are formulated, respectively, for the in-plane state (membrane) and for the out-of-plane state (bending). These uncoupled systems are joined to form a macro-element, in which membrane and bending effects are present. The association of these macro-elements is able to simulate thin-walled structures, including reinforced plate structures. In the present formulation, the BIE is discretized by continuous and/or discontinuous linear elements. Four displacement integral equations are written for every boundary node. Modal data, that is, natural frequencies and the corresponding mode shapes of reinforced plates, are obtained from information contained in the frequency response functions (FRFs). A specific example is presented to illustrate the versatility of the proposed methodology. Different configurations of the reinforcements are used to simulate simply supported and clamped boundary conditions for the plate structures. The procedure is validated by comparison with results determined by the finite element method (FEM).

1. Introduction

Reinforced panel systems are widely used in buildings, bridges, ships, aircrafts, and machines. These structural systems are efficient, economical, and readily constructed from common materials. The panels are usually built by the association of plates (or shells)

with orthogonally displaced beams, which are the reinforcements. The main advantage of applying these structural elements is the increase of structural rigidity without considerable increase in weight.

The static analysis of the reinforced plate systems has been performed using solution strategies such as methodologies based on energy principles [1], semi-analytical methods [2], or the differential quadrature methods [3]. Also it is possible to model the behavior of these structures by the finite element method (FEM) [4, 5], the boundary element method (BEM) [6–10], or a combination of these numerical methods [11]. A rather limited amount of technical literature is available on the dynamic analysis of stiffened plate systems. On the other hand, a significant research effort is under way in both the academia and the industry to improve the numerical models and to develop new modeling methods for the dynamic analysis [12]. Finite and boundary elements have some limitations to obtain vibration responses at middle and upper frequency ranges due to the necessity of intense mesh refining. The use of very fine meshes in the finite element analysis results in large algebraic systems. An alternative is posed by the BEM. If formulated with the proper auxiliary state, the BEM only requires boundary discretization, leading to considerable smaller algebraic systems.

Direct boundary element subregion formulations based on Kirchhoff's plate theory has been applied to the dynamic analysis of thin-walled structures formed by assembling folded plate models using the so-called static fundamental solution [13, 14]. Assembled plate structures were also analyzed by BEM and comparisons with FEM are given to demonstrate the accuracy of this methodology [15]. Another dynamic analysis of elastic plates reinforced with beams takes into account the resulting in-plane forces and deformations in the plate, as well as the axial forces and deformations in the beam, due to combined response of the system [16]. The method presented in [16] employs the static solution similar to the models described previously. The consequence of these formulations is that the inertia forces lead to domain integrals. In these previous articles, it was necessary to develop a procedure to deal with the domain integral. An alternative way to derive the governing integral equation for the problem is to use a stationary dynamic fundamental solution [17–19]. If this fundamental solution is applied, the resulting integral equation requires only the discretization of the boundary of the single-folded plate being analyzed.

The present paper analyzes the dynamic stationary response of reinforced panels subjected to time harmonic loadings using the BEM. In the proposed methodology, the panels are considered as assembled folded-plate structures [20]. The formulation is built by coupling BE formulations of plate bending and two-dimensional plane stress elasticity. These uncoupled systems are joined to form a macro-element. The plate structure is divided into several regions, and equilibrium and compatibility equations along the interface boundaries are imposed. The boundaries are discretized by means of linear continuous and discontinuous isoparametric elements. Four displacement integral equations are written for every boundary node. The stationary dynamic responses are characterized by modal quantities, that means by eigenfrequencies and eigenvalues. These quantities are obtained by analyzing the numerically synthesized frequency response functions (FRFs) of the reinforced structures. A harmonic force of constant amplitude excites the

structure at a given point and the resulting displacement is measured (calculated) at another point. From the resonances or peaks of the FRFs, the operational eigenfrequencies may be determined. The operational eigemodes (vibration mode shapes) are determined by calculating the folded-plate structure displacement field at the determined operational eigenfrequencies. In the present article, an example is presented to illustrate the proposed methodology where different configurations of the reinforcements are used to simulate simply supported and clamped boundary conditions. The implementation is validated by comparison with numerical results determined by FE solutions. The results obtained by the present BEM are shown to be in good agreement with those obtained by the FEM. The proposed scheme may be seen as an accurate methodology to analyze free and forced stationary vibrations of structures assembled by folded plates, like plate structures and reinforced panels. This methodology may be regarded as an extension of the previous article that analyzed the stationary dynamic behavior of frame structures by the BEM [21].

2. Boundary integral formulations

The dynamic equilibrium equations for plane stress and thin plate theory will be presented next with Latin indices taking values {1, 2, and 3} and Greek indices assuming the range {1, 2}. In the plane macro-element formulation, the membrane displacements u_1 and u_2 are in the x_1-x_2 plane. The thin plate transversal displacement w is in the x_3 directions. The equilibrium equations for the dynamic plane stress problem in the domain Ω is given by

$$\sigma_{\alpha\beta,\beta} + \rho F_\alpha = \rho \ddot{u}_\alpha, \tag{2.1}$$

where σ_{ij} represents the stresses components, ρ is the mass density, F_α $(\alpha = 1,2)$ are the body forces components in the x_1-x_2 plane and dots over the quantities indicate differentiation with respect to time.

The equilibrium equations for an infinitesimal thin plate element under a dynamical transverse loading g and in absence of a body forces are given by

$$\begin{aligned} q_{\alpha,\alpha} + g &= \rho h \ddot{w}, \\ m_{\alpha\beta,\beta} - q_\alpha &= 0, \end{aligned} \tag{2.2}$$

where ρh is the mass density per unit area, h is the thickness, $q_\alpha(q_1, q_2)$ represent the shear forces, $m_{\alpha\alpha}(m_{11}, m_{22})$ represent the bending moments and $m_{\alpha\beta}(m_{12}, m_{21})$ represent the twisting moments.

Now consider the plane element occupying the area Ω, bounded by the contour Γ, in the plane x_1-x_2. The displacement boundary integral equation for the plane stressproblem

(membrane) and smooth boundaries is given by

$$\frac{1}{2}\delta_{\alpha\beta}u_\beta(P) = \int_\Gamma U^*_{\alpha\beta}(P,Q)t_\beta(Q)d\Gamma(Q) - \int_\Gamma T^*_{\alpha\beta}(P,Q)u_\beta(Q)d\Gamma(Q) + \int_\Omega U^*_{\alpha\beta}(P,Q)F_\beta(Q)d\Omega(Q), \tag{2.3}$$

where $\delta_{\alpha\beta}$ is the *Kronecker* delta; $d\Gamma$ and $d\Omega$ denote boundary and domain differentials, respectively; $u_\beta(Q)$ and $t_\beta(Q)$ are displacement and traction boundary values associated with a boundary point Q, respectively. The term $U^*_{\alpha\beta}(Q,P)$ represents a displacement fundamental solution and may be interpreted as the displacement at point Q in the direction α due to a harmonic unit point force applied at the point P in the direction β. Analogosly, the term $T^*_{\alpha\beta}(Q,P)$ represents the traction fundamental solution and may also be interpreted as the traction at point Q in the direction α due to a harmonic unit point load applied at P in the direction β.

Considering that all variables are undergoing a time harmonic displacement with circular frequency ω, the displacement and traction fundamental solutions are given, respectively, by the expressions [22]

$$U^*_{\alpha\beta} = \frac{1}{2\pi\rho c_2^2}\left[\psi\delta_{\alpha\beta} - \chi r_{,\alpha}r_{,\beta}\right], \tag{2.4}$$

where

$$\begin{aligned}
\psi &= K_0(k_2r) + \frac{1}{k_2r}\left[K_1(k_2r) - \frac{c_2}{c_1}K_1(k_1r)\right],\\
\chi &= K_2(k_2r) - \frac{c_2^2}{c_1^2}K_2(k_1r),\\
T^*_{\alpha\beta} &= \frac{1}{2\pi}\left[\left(\frac{d\psi}{dr} - \frac{1}{r}\chi\right)\left(\delta_{\alpha\beta}\frac{\partial r}{\partial n} + r_{,\beta}n_\alpha\right) - \frac{2}{r}\chi\left(n_\beta r_{,\alpha} - 2r_{,\alpha}r_{,\beta}\frac{\partial r}{\partial n}\right)\right.\\
&\quad \left. - 2\frac{d\chi}{dr}r_{,\alpha}r_{,\beta}\frac{\partial r}{\partial n} + \left(\frac{c_1^2}{c_2^2} - 2\right)\left(\frac{d\psi}{dr} - \frac{d\chi}{dr} - \frac{1}{r}\chi\right)r_{,\alpha}n_\beta\right],
\end{aligned} \tag{2.5}$$

where $\delta_{\alpha\beta}$ is again the *Kronecker* delta, n is the normal vector, K_0 and K_1 are the zero and first-order modified *Bessel* function of second kind, r is the distance between load and displacement point, $k_1 = i(\omega/c_1)$ and $k_2 = i(\omega/c_2)$, $i = \sqrt{-1}$, ω is the circular frequency, $c_1 = (\lambda + 2\mu/\rho)^{1/2}$, $c_2 = (\mu/\rho)^{1/2}$, λ and μ are the *Lamé's* constants which can be written in terms of the *Young* Modulus E and the Poisson ratio ν.

Additionally, the integral equation for the thin plate theory is employed to describe the bending action:

$$\begin{aligned}\frac{1}{2}\delta(P)w(P)+\int_{\Gamma}\left[V_n^*(P,Q)w(Q)-M_n^*(P,Q)w_{,n}(Q)\right]d\Gamma(Q)+\sum_{k=1}^{N_c}R_{ck}^*(P,c)w_{ck}(P,c)\\ =\int_{\Gamma}\left[w^*(P,Q)V_n(Q)-w_{,n}^*(P,Q)M_n(Q)\right]d\Gamma(Q)\\ +\sum_{k=1}^{N_c}w_{ck}^*(P,Q)R_{ck}(Q)+\int_{\Omega}w^*(P,q)g(q)d\Omega(q),\end{aligned}\tag{2.6}$$

where $\delta(P)$ is equal to *Kronecker* delta for a smooth boundary, w is the out-of-plane displacement, $w_{,n}$ is the rotation in the direction of outward normal to the boundary Γ, V_n is the equivalent shear, M_n is the bending moment, and R_c is the corner reaction. The classical theory makes use of the equivalent shear (V_n) in boundary integrals and a corner reaction (R_c) at each corner when polygonal plates are considered,

$$V_n=Q_n+\frac{\partial M_{ns}}{\partial s}=-D\left(w_{,\gamma\gamma\alpha}\cdot n_\alpha+(1-\nu)w_{,nss}\right)\tag{2.7}$$

$$R_{ck}=\left(M_{ns}^F-M_{ns}^B\right)_k,\tag{2.8}$$

where Q_n is the shear in the direction of outward normal and M_{ns} is the twisting moment in the direction normal and tangential to the boundary Γ. The expression (2.8) presents the corner reaction (R_c) at corner k as the difference between the twisting moments at the corner neighborhood on the forward side (M_{ns}^F) and the backward side (M_{ns}^B).

Considering again that all variables are undergoing a time harmonic displacement, $u(t)=\hat{u}\exp(i\omega t)$ with circular frequency ω. Under this circumstance, load g and deflections w will also vary harmonically and the fundamental solution for (2.6) has the form [23, 24]

$$w^*=-iC_1J_0(\eta r)+C_1Y_0(\eta r)+C_2K_0(\eta r)\tag{2.9}$$

with

$$C_1=\frac{1}{8\eta^2},\qquad C_2=\frac{1}{4\pi\eta^2},\qquad \eta^4=\frac{\rho h\omega^2}{D}.\tag{2.10}$$

In (2.9) to (2.10), the flexural rigidity D is equal to $Eh^3/[12(1-\nu^2)]$, E is the *Young* Modulus and ν is the Poisson ratio. The variables J_0 and Y_0 are the zero-order *Bessel* functions of the first and second kind, respectively, K_0 is the zero-order modified *Bessel*

function of the second kind. Explicit expressions for derivatives of fundamentals solutions, rotations $w^*_{,n}$, moments M^*_n, and shear forces V^*_n are as follows [23]:

$$
\begin{aligned}
w^*_{,n} &= iC_1\eta J_1(\eta r)\cos\overline{\beta} - \eta\left[C_1Y_1(\eta r) + C_2K_1(\eta r)\right]\cos\overline{\beta},\\
M^*_n &= -i\left\{C_1\frac{D}{2}\left[1+\nu+(1-\nu)\cos 2\overline{\beta}\right]\eta^2 J_0(\eta r) - C_1D\eta(1-\nu)\frac{J_1(\eta r)}{r}\cos 2\overline{\beta}\right\}\\
&\quad + \frac{D}{2}\left\{\eta^2\left[1+\nu+(1-\nu)\cos 2\overline{\beta}\right]\left[C_1Y_0(\eta r) - C_2K_0(\eta r)\right]\right.\\
&\qquad \left. - 2\eta(1-\nu)\frac{1}{r}\left[C_1Y_1(\eta r) + C_2K_1(\eta r)\right]\cos 2\overline{\beta}\right\},\\
V^*_n &= iC_1D\left\{J_1(\eta r)\left[\eta^3\cos\overline{\beta} + \frac{\eta^3(1-\nu)}{2}\operatorname{sen}2\overline{\beta}\operatorname{sen}\overline{\beta} + \frac{2\eta(1-\nu)}{r}\left(\frac{\cos 3\overline{\beta}}{r} - \frac{\cos 2\overline{\beta}}{R}\right)\right]\right.\\
&\qquad \left. + (1-\nu)\eta^2 J_0(\eta r)\left(\frac{\cos 2\overline{\beta}}{R} - \frac{\cos 3\overline{\beta}}{r}\right)\right\} - D\eta^3\left[C_1Y_1(\eta r) - C_2K_1(\eta r)\right]\cos\overline{\beta}\\
&\quad + D(1-\nu)\left\{\frac{\eta^2}{r}\left[C_1Y_0(\eta r) - C_2K_0(\eta r)\right] - \frac{2\eta}{r^2}\left[C_1Y_1(\eta r) + C_2K_1(\eta r)\right]\cos 3\overline{\beta}\right\}\\
&\quad - D(1-\nu)\left\{\frac{\eta^2}{R}\left[C_1Y_0(\eta r) - C_2K_0(\eta r)\right] - \frac{2\eta}{rR}\left[C_1Y_1(\eta r) + C_2K_1(\eta r)\right]\cos 2\overline{\beta}\right\}\\
&\quad - \frac{D(1-\nu)}{2}\eta^3\left[C_1Y_1(\eta r) - C_2K_1(\eta r)\right]\operatorname{sen}2\overline{\beta}\operatorname{sen}\overline{\beta},
\end{aligned}
\tag{2.11}
$$

where J_1 and Y_1 are the first-order *Bessel* functions of the first and second kind, respectively; K_1 is the first-order modified *Bessel* function of the second kind and $\overline{\beta}$ the angle formed between r and n.

3. Algebraic formulation of the macro-elements

In this session, the plane macro-element will be assembled by superposition of the membrane and thin plate effects. The plane stress boundary integral equation (2.3) representing the membrane may be discretized leading to the following algebraic system of equations:

$$
\begin{bmatrix} H^m_{11} & H^m_{12} \\ H^m_{21} & H^m_{22} \end{bmatrix}
\begin{Bmatrix} u_1 \\ u_2 \end{Bmatrix}
=
\begin{bmatrix} G^m_{11} & G^m_{12} \\ G^m_{21} & G^m_{22} \end{bmatrix}
\begin{Bmatrix} t_1 \\ t_2 \end{Bmatrix}.
\tag{3.1}
$$

Analogosly, the BIE (2.6) describing the out-of-plane bending effect (thin plate) may be discretized as follows:

$$
\begin{bmatrix} H^p_{11} & H^p_{12} \\ H^p_{21} & H^p_{22} \end{bmatrix}
\begin{Bmatrix} w \\ w_{,n} \end{Bmatrix}
=
\begin{bmatrix} G^p_{11} & G^p_{12} \\ G^p_{21} & G^p_{22} \end{bmatrix}
\begin{Bmatrix} V_n \\ M_n \end{Bmatrix}.
\tag{3.2}
$$

In (3.1) and (3.2), the upper indices m and p on the coefficient matrices H and G stand, respectively, for membrane and plate mechanisms. Furthermore, u_1 and u_2 represent the

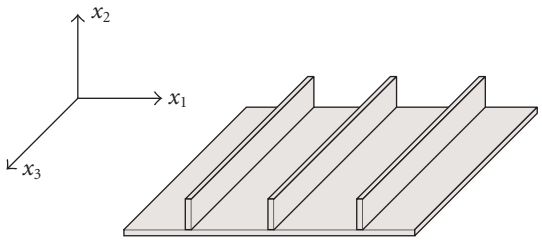

Figure 3.1. Global coordinate system and macro-elements interfaces.

in-plane membrane displacements associated with the in-plane tractions t_1 and t_2. The plate displacement normal to the x_1-x_2 plane is w and its derivative with respect to the boundary normal n is $w_{,n}$. The corresponding generalized forces are the shear forces V_n and the bending moment M_n. Equations (3.1) and (3.2) may be superposed to form the plane macro-element in which membrane and bending mechanisms are uncoupled:

$$\begin{bmatrix} H_{11}^m & H_{12}^m & 0 & 0 \\ H_{21}^m & H_{22}^m & 0 & 0 \\ 0 & 0 & H_{11}^p & H_{12}^p \\ 0 & 0 & H_{21}^p & H_{22}^p \end{bmatrix} \begin{Bmatrix} u_1 \\ u_2 \\ w \\ w,n \end{Bmatrix} = \begin{bmatrix} G_{11}^m & G_{12}^m & 0 & 0 \\ G_{21}^m & G_{22}^m & 0 & 0 \\ 0 & 0 & G_{11}^p & G_{12}^p \\ 0 & 0 & G_{21}^p & G_{22}^p \end{bmatrix} \begin{Bmatrix} t_1 \\ t_2 \\ V_n \\ M_n \end{Bmatrix}. \tag{3.3}$$

The interface boundaries between macro-elements must be parallel to a single axis. In a global coordinate system, this axis is called x_3, as shown in Figure 3.1. Figure 3.1 also shows a plate with reinforcements. It can be noticed that the reinforcements are all aligned parallel to the x_3 axis.

The plane macro-element given by (3.3) is written in terms of a local coordinate system. To perform the coupling of distinct macro-elements, as the ones shown in Figure 3.1, it is necessary to transform (3.3) from a local to a global coordinate system. This is done by means of an intermediate coordinate system and a set of two coordinate transformation matrices. After the macro-element equations have been written in terms of the global coordinate system, the assemblage may take place. The vector of generalized displacements and forces may now be subdivided into ones belonging or not to a common interface. For the case of two macro-elements, the individual equations for every macro-element may be written as

$$\begin{bmatrix} H_{11}^1 & H_{1i}^1 \\ H_{i1}^1 & H_{ii}^1 \end{bmatrix} \begin{Bmatrix} U_1 \\ U_i^1 \end{Bmatrix} = \begin{bmatrix} G_{11}^1 & G_{1i}^1 \\ G_{i1}^1 & G_{ii}^1 \end{bmatrix} \begin{Bmatrix} T_1 \\ T_i^1 \end{Bmatrix},$$
$$\begin{bmatrix} H_{11}^2 & H_{1i}^2 \\ H_{i1}^2 & H_{ii}^2 \end{bmatrix} \begin{Bmatrix} U_2 \\ U_i^2 \end{Bmatrix} = \begin{bmatrix} G_{11}^2 & G_{1i}^2 \\ G_{i1}^2 & G_{ii}^2 \end{bmatrix} \begin{Bmatrix} T_2 \\ T_i^2 \end{Bmatrix}. \tag{3.4}$$

The coupling of the macro-elements is performed by considering kinematic compatibility and equilibrium at the interface nodes. Considering T the vector of external loads

applied at the elements interface, compatibility and equilibrium is given by

$$\begin{aligned} U_i^1 &= U_i^2 = U_i, \\ T_i^1 + T_i^2 + T &= 0. \end{aligned} \tag{3.5}$$

After (3.5) has been applied to (3.4), the basic system of equation for two coupled macro-elements is given by

$$\begin{bmatrix} H_{11}^1 & H_{1i}^1 & 0 & -G_{1i}^1 & 0 \\ H_{i1}^1 & H_{ii}^1 & 0 & -G_{ii}^1 & 0 \\ 0 & H_{ii}^2 & H_{i2}^2 & 0 & -G_{ii}^2 \\ 0 & H_{2i}^2 & H_{22}^2 & 0 & -G_{2i}^2 \\ 0 & 0 & 0 & I & I \end{bmatrix} \begin{Bmatrix} U_1 \\ U_i \\ U_2 \\ T_i^1 \\ T_i^2 \end{Bmatrix} = \begin{bmatrix} G_{11}^1 & 0 & 0 \\ G_{1i}^1 & 0 & 0 \\ 0 & 0 & G_{i2}^2 \\ 0 & 0 & G_{22}^2 \\ 0 & I & 0 \end{bmatrix} \begin{Bmatrix} T_1 \\ T \\ T_2 \end{Bmatrix}. \tag{3.6}$$

In (3.6), U_1 and U_2 are generalized displacement vectors (bending and stretching) related to subregions Ω_1 and Ω_2, respectively. T_1 and T_2 are the corresponding generalized forces. The displacement vector U_i and the corresponding forces vector T_i stand for the values at the interface; T_i^1 and T_i^2 represent forces vectors at the interfaces for each one of the macro-elements.

4. BEM formulations

In this paper, the macro-elements coupled by (3.6) were discretized by rectilinear boundary elements described by linear shape functions. Considering B_1 and B_2 the initial and final coordinates of the elements, the element geometry may be expressed in terms of intrinsic coordinates, ς:

$$b(\varsigma) = B_1 \frac{1-\varsigma}{2} + B_2 \frac{1+\varsigma}{2}. \tag{4.1}$$

This same interpolation is used for the field variables of the boundary elements possessing no corners, leading to an isoparametrical formulation. For elements with corners, the field variables were discretized by discontinuous elements. The corner nodes were displaced towards the interior by one-fourth of the element length ($0.25\,L_e$). Four integral equations were written for every boundary node. The collocation points were placed outside the plane element (macro-element) domains. When collocation point P is placed outside the plate domain ($P \notin \Omega$), the integration free-term disappears, $\delta(P) = 0$. Moreover, the corner reactions R_{ck} can be written in terms of neighbor node rotations using a finite difference scheme. Although this is the correct way to treat corner reactions, in the present implementation these terms were neglected.

A final algebraic system $[A]\{X\} = \{B\}$ is obtained once the equations are assembled and the prescribed boundary conditions applied. The solution of this system, the vector X, contains all unknown boundary quantities. The system matrix $[A(\omega)]$ contains frequency dependent terms. After the vector X is determined, the displacement at the assembled folded plate domains may be readily obtained by the nonsingular integrations indicated in (2.3) and (2.6).

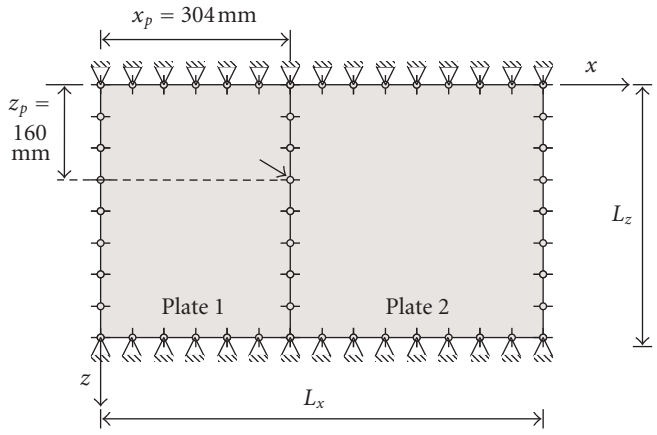

Figure 5.1. Two plates, S-F-S-F, no reinforcements.

5. Numerical analysis

This session applies the previously described strategy to analyze reinforced panels. The strategy is simple. Consider two joined rectangular plates, simply supported (S) in two edges $z = 0$ and $z = L_z$, and freely supported (F) at the remaining edges, $x = 0$ and $x = L_x$, as shown in Figure 5.1. The plates are excited by a concentrated force applied at the point with coordinates x_p and z_p. The frequency of excitation is continuously changed within a preestablished range. The displacement response at some point of the plates to this frequency dependent excitation is the so-called frequency response function (FRF).

In the sequence, reinforcements are placed at the boundaries $x = 0$ and $x = L_x$. If the reinforcement is very thin but very high in the y-direction, then the bending effect of the support is very small compared to the membrane effect. This should simulate a simply supported (S) boundary condition. On the other hand, if the plate thickness is increased, then the clamped (C) boundary condition should be simulated. The validation strategy is composed of these three steps. In the first step, the FRF of S-F-S-F plate is determined and the natural frequencies of the present methodology compared to results from a finite element (FE) analysis. In the second step, high but thin reinforcements are placed at the originally free boundaries, giving rise to a model that simulates completely simply supported plates S-S-S-S. Again the operational eigenfrequencies are obtained from the FRF. Comparisons are also made with the FE solution. Finally, thicker reinforcements are placed at the free boundaries, simulating the clamped (C) boundary condition. The operational eigenfrequencies for this C-S-C-S plate are compared to the FE results. This strategy is sketched in Figure 5.2.

Take initially the two plates loaded by a unit harmonic normal excitation on the interface between the two plates at distances $x_1 = 304\,\text{mm}$ and $x_3 = 160\,\text{mm}$ (X-Z plane), as shown in Figure 5.1. The two plates are assembled and are simply supported (S) at their edges $z = 0$ and $z = L_z$, andfree (F) at their boundaries $x = 0$ and $x = L_x$. Each

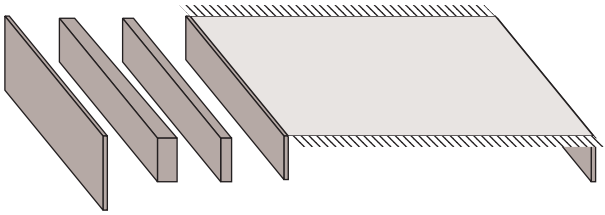

Figure 5.2. Reinforcements as replacements for distinct boundary conditions.

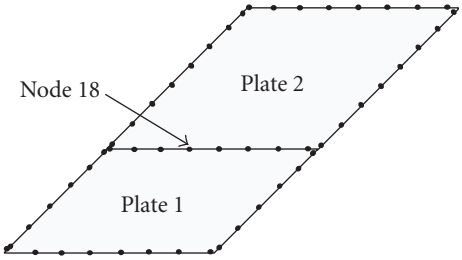

Figure 5.3. Example of the discretization for the two plates.

Table 5.1. First six natural frequencies of the two SFSF plates [Hz].

Method	Mesh	ω_1	ω_2	ω_3	ω_4	ω_5	ω_6
BEM	1	6056	7618	12 110	19 922	24 415	26 172
	2	6056	7618	12 305	20 313	24 415	26 172
FEM	1	5951	7459	12 013	19 709	23 878	25 575

assembled plate is made of same constitutive properties with Young's modulus $E = 6.9 \times 10^{10}\,\text{kN/m}^2$, thickness $h = 4\,\text{mm}$, density $\rho = 2700\,\text{Kg/m}^3$, length $L_x = 704\,\text{mm}$, width $L_z = 400\,\text{mm}$, and Poisson ratio $\nu = 0.3$.

Computations by the BEM are carried out for the following boundary discretization (two macro-elements) using linear micro-elements: Mesh 1 : 18 and 20 boundary elements per macro-element (plate 1 and 2, resp.) and Mesh 2 : 28 and 30 boundary elements per macro-element (plate 1 and 2, resp.). An example of the discretization of boundary is shown in Figure 5.3.

Figure 5.4 shows the $\text{FRF}_{18\text{-}18}$ for the first BEM mesh. The $\text{FRF}_{18\text{-}18}$ is obtained by exciting node 18 (see Figure 5.3) and measuring the response at the same node. In this FRF, the resonances and antiresonances can be clearly recognized. The system operational eigenfrequencies (natural frequencies) are determined from the frequencies at which resonances in the FRF occur.

The values of the first six eigenfrequencies taken from the FRF of the two assembled plates given in Figure 5.4 are reproduced in Table 5.1. These valuesare compared with

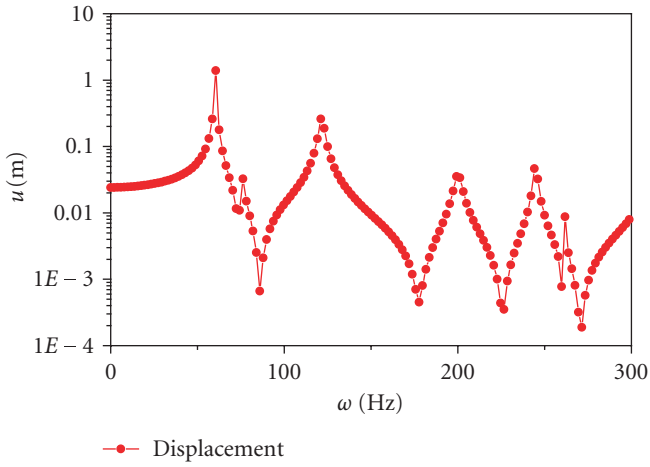

Figure 5.4. $FRF_{18\text{-}18}$ for the first BE discretization of the two SFSF plates.

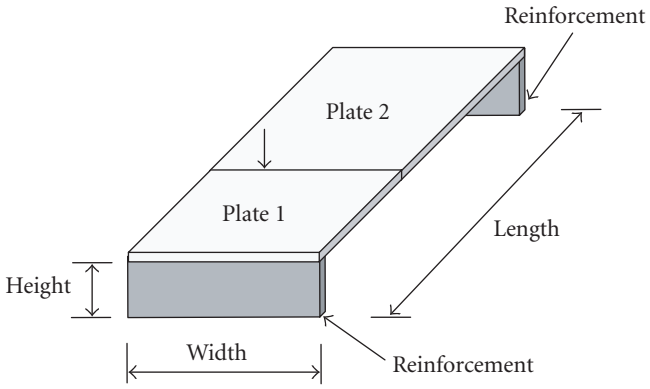

Figure 5.5. Reinforced panel structure subjected to concentrated time-harmonic load.

similar discretization of the FEM by ANSYS® using SHELL63® elements. The discretization of de FEM by ANSYS® consisted of the 18×30 finite elements.

Now the reinforcements are included in the originally freely supported boundary conditions (F). The resulting reinforced panel structure is shown in Figure 5.5. In the reinforcements, only the central nodes of the sides are submitted to simply supported boundary conditions. The remaining nodes are free.

To simulate a simply supported boundary condition (S) as shown in Figure 5.6, the reinforcement is a thin and high macro-element. In this case, the plates and reinforcements are made of same material properties described in the previous example.

The reinforced panel is discretized with 4 macro-elements, 2 elements for the plates and 2 elements for the reinforcements (see Figure 5.7). Two BE meshes are used to perform the calculations. In the first mesh, all 4 macro-elements are discretized with 18×20

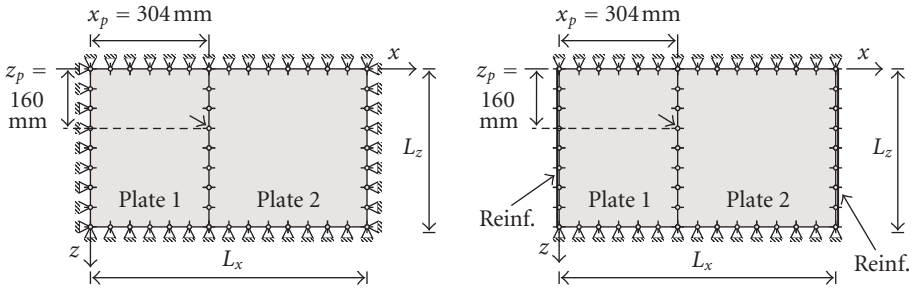

(a) Boundary conditions (S-S-S-S) (b) Equivalent thin reinforcements

Figure 5.6. Schematic illustration of the reinforced panel structure.

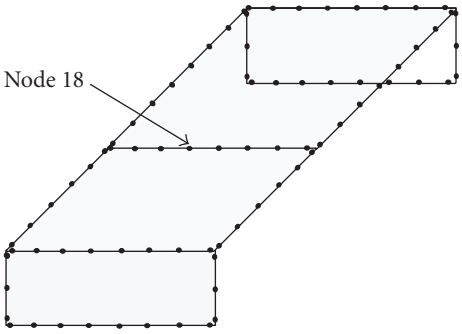

Figure 5.7. BEM for the reinforced panel structure (Mesh 1).

Table 5.2. First six natural frequencies of the SSSS structure [Hz].

Method	Mesh	ω_1	ω_2	ω_3	ω_4	ω_5	ω_6
BEM	1	8203	14063	24024	26563	32617	37891
	2	8203	14 063	24 024	26 563	32 617	37 891
FEM	1	7911	13 638	23 174	25 771	31 292	36 528

linear elements. In the second mesh, the 4 macro-elements have been discretized with 28×30 linear elements. The geometric properties of the reinforcements are thickness 0.4 mm, height 400 mm, and width 400 mm.

The $\text{FRF}_{18\text{-}18}$, of the reinforced panel structure is shown in Figure 5.8, for the discretization (Mesh 1) mentioned above.

The values of the first six eigenfrequencies of the reinforced panel structure are reproduced in Table 5.2. These values are compared with results obtained by the FEM commercial code ANSYS® using 18×30 SHELL63® elements.

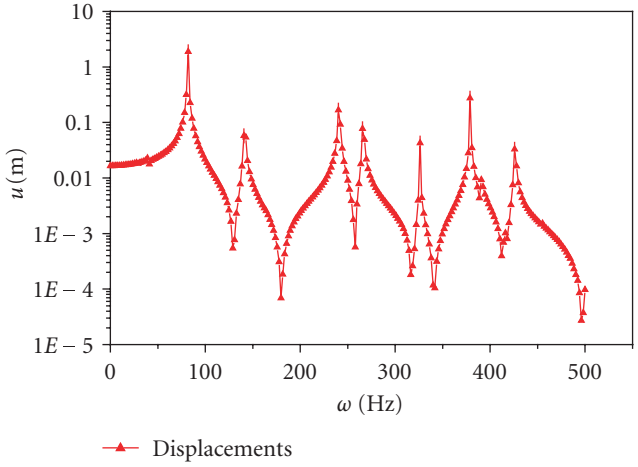

Figure 5.8. $FRF_{18\text{-}18}$ for the first BEM discretization of the reinforced SSSS panel.

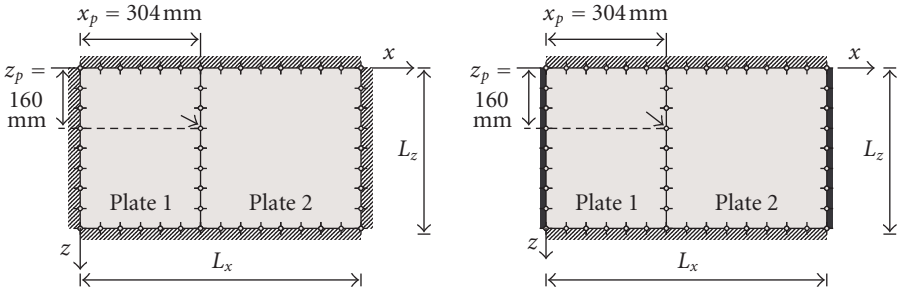

Figure 5.9. Scheme to reproduce clamped boundary conditions on the plate by thick reinforcements.

Let us now consider the plate structure with its entire contour under clamped (C) boundary conditions (Figure 5.9(a)). The intention is to simulate a clamped boundary condition of the two plates on the boundaries $z = 0$ and $z = L_z$ using a thick reinforcement. The idea was to introduce thick reinforcements to increase the bending rigidity. This strategy is illustrated in Figure 5.9(b). In the reinforcement, only the central nodes of the sides are considered clamped. The others are considered free. In this case, the plates are made of same material properties and geometry described in the previous example. However, the thickness of the two reinforcements is increased to 40 mm. This thickness is increased by a factor 100, compared to the previous case.

The $FRF_{18\text{-}18}$, of the reinforced (campled) panel structure discretized by BE is shown in Figure 5.10. The discretization utilized is the same as the previous case (mesh 1).

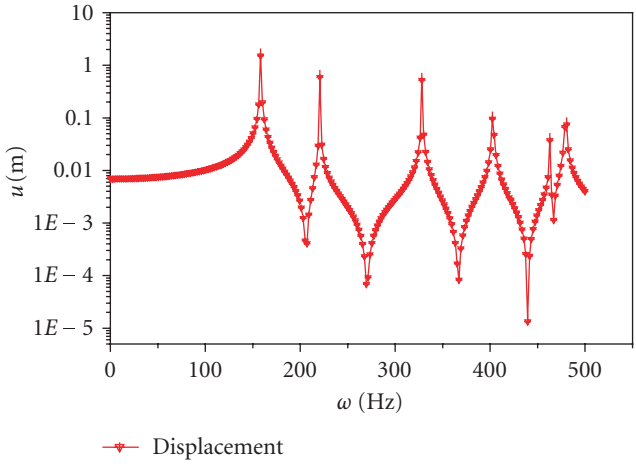

Figure 5.10. $FRF_{18\text{-}18}$ for the first BEM discretization of the reinforced CCCC panel.

Table 5.3. First six natural frequencies of the CCCC structure [Hz].

Method	Mesh	ω_1	ω_2	ω_3	ω_4	ω_5	ω_6
BEM	1	15 821	22 071	32 813	40 235	46 289	48 046
FEM	1	15 456	21 485	32 019	39 328	45 023	46 860

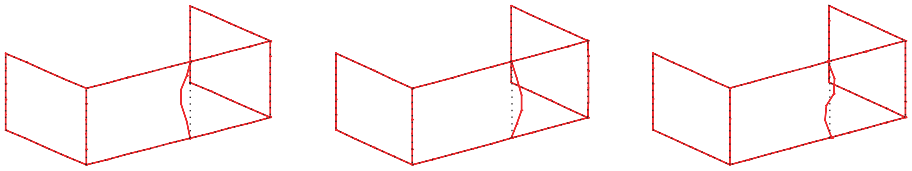

(a) $\omega_1 = 15821$ Hz (b) $\omega_2 = 22071$ Hz and $\omega_3 = 32813$ Hz (c) $\omega_4 = 40235$ Hz

Figure 5.11. Four lower operational eigenmodes for the CCCC structure.

The values of the first six (operational) eigenfrequencies are reproduced in Table 5.3. The eigenvalues obtained by the commercial FEM code ANSYS® using 18×30 SHELL63® elements are also given in Table 5.3.

The other modal quantity necessary to characterize the stationary dynamic behavior of the reinforced panel structure is given by the eigenmodes or the natural modes of vibration. For the last case (clamped bc), the operational eigenmodes are obtained by calculating the displacement field at boundary of the structure at each resonance frequency present in the FRF.

Figure 5.11 shows the boundary displacements corresponding to the first four eigenmodes of the excited structure. In this case, all external boundary nodes of the structure are campled. It should be noticed that the second and third modes present the same boundary displacement.

6. Concluding remarks

An implementation of the direct version of the boundary element method has been presented to analyze the stationary dynamic behavior of the reinforced panel structures. The dynamic stationary fundamental solution has been used to transform the differential equations governing the thin plate and membrane behavior into boundary-only integral equations. The proposed scheme is used, exemplarily, to obtain modal data, that is, operational eigenfrequencies and eigenmodes of the assembled plates and reinforced panel structures with different boundary conditions. The formulation was shown to be capable of modelling plates subjected to varied boundary conditions and out-of-plane loadings. Frequency response functions may be determined for every boundary or domain point of the structure. In the reported examples, the FRF of a node on an interface boundary is used to recover eigenfrequencies. The eigenfrequencies are determined from the resonances of the FRF. At these resonance frequencies, the displacement fields of the structure furnish the operational eigenmodes. The presented results agree well with numerical solutions obtained by a FEM commercial code. The proposed scheme may be seen as an accurate methodology to analyze free and forced stationary vibrations of structures assembled by folded plates, plate structures, and also reinforced panels which only require the discretization of the folded plate boundary. The simplicity of the BE mesh generation presents some advantages over other domain methods.

Acknowledgment

The research leading to this article has been supported by FAPESP. This is gratefully acknowledged.

References

[1] A. R. Kukreti and E. Cheraghi, "Analysis procedure for stiffened plate systems using an energy approach," *Computers & Structures*, vol. 46, no. 4, pp. 649–657, 1993.

[2] M. Mukhopadhyay, "Stiffened plates in bending," *Computers & Structures*, vol. 50, no. 4, pp. 541–548, 1994.

[3] Z. A. Siddiqi and A. R. Kukreti, "Analysis of eccentrically stiffened plates with mixed boundary conditions using differential quadrature method," *Applied Mathematical Modelling*, vol. 22, no. 4-5, pp. 251–275, 1998.

[4] A. Deb and M. Booton, "Finite element models for stiffened plates under transverse loading," *Computers & Structures*, vol. 28, no. 3, pp. 361–372, 1988.

[5] G. S. Palani, N. R. Iyer, and T. V. S. R. Appa Rao, "An efficient finite element model for static and vibration analysis of eccentrically stiffened plates/shells," *Computers & Structures*, vol. 43, no. 4, pp. 651–661, 1992.

[6] M. Tanaka and A. N. Bercin, "A boundary element method applied to the elastic bending problem of stiffened plates," in *Proceedings of the 19th International Conference on Boundary Element Methods (BEM '97)*, pp. 203–212, Rome, Italy, September 1997.

[7] E. J. Sapountzakis and J. T. Katsikadelis, "Analysis of plates reinforced with beams," *Computational Mechanics*, vol. 26, no. 1, pp. 66–74, 2000.

[8] M. Tanaka, T. Matsumoto, and S. Oida, "A boundary element method applied to the elastostatic bending problem of beam-stiffened plates," *Engineering Analysis with Boundary Elements*, vol. 24, no. 10, pp. 751–758, 2000.

[9] P. H. Wen, M. H. Aliabadi, and A. Young, "Boundary element analysis of shear deformable stiffened plates," *Engineering Analysis with Boundary Elements*, vol. 26, no. 6, pp. 511–520, 2002.

[10] L. de Oliveira Neto and J. B. de Paiva, "A special BEM for elastostatic analysis of building floor slabs on columns," *Computers & Structures*, vol. 81, no. 6, pp. 359–372, 2003.

[11] S. F. Ng, M. S. Cheung, and T. Xu, "A combined boundary element and finite element solution of slab and slab-on-girder bridges," *Computers & Structures*, vol. 37, no. 6, pp. 1069–1075, 1990.

[12] J. R. F. Arruda and K. M. Ahmida, "The structural dynamics mid-frequency challenge: bridging the gap between FEA and SEA," in *Proceedings of the 10th International Symposium on Dynamic Problems of Mechanics (DINAME '03)*, pp. 159–164, ABCM, Ubatuba, Brazil, March 2003.

[13] M. Tanaka, K. Yamagiwa, K. Miyazaki, and T. Ueda, "Free vibration analysis of elastic plate structures by boundary element method," *Engineering Analysis*, vol. 5, no. 4, pp. 182–188, 1988.

[14] M. Tanaka, T. Matsumoto, and A. Shiozaki, "Application of boundary-domain element method to the free vibration problem of plate structures," *Computers & Structures*, vol. 66, no. 6, pp. 725–735, 1998.

[15] T. Dirgantara and M. H. Aliabadi, "Boundary element analysis of assembled plate structures," *Communications in Numerical Methods in Engineering*, vol. 17, no. 10, pp. 749–760, 2001.

[16] E. J. Sapountzakis and J. T. Katsikadelis, "Dynamic analysis of elastic plates reinforced with beams of doubly-symmetrical cross section," *Computational Mechanics*, vol. 23, no. 5, pp. 430–439, 1999.

[17] D. E. Beskos, "Boundary element methods in dynamic analysis," *Applied Mechanics Reviews*, vol. 40, no. 1, pp. 1–23, 1987.

[18] D. E. Beskos, "Dynamic analysis of plates," in *Boundary Element Analysis of Plates and Shells*, D. E. Beskos, Ed., pp. 35–92, Springer, Berlin, Germany, 1991.

[19] D. E. Beskos, "Boundary element methods in dynamic analysis—part II (1986–1996)," *Applied Mechanics Reviews*, vol. 50, no. 3, pp. 149–197, 1997.

[20] L. C. F. Sanches, E. Mesquita, and L. Palermo Jr., "The dynamic of thin-walled structures by the boundary element method," in *Proceedings of the 25th CILAMCE: 25nd Iberian Latin-American Congress on Computational Methods in Engineering*, Campinas, Brazil, 2004.

[21] E. Mesquita, S. F. A. Barretto, and R. Pavanello, "Dynamic behavior of frame structures by boundary integral procedures," *Engineering Analysis with Boundary Elements*, vol. 24, no. 5, pp. 399–406, 2000.

[22] J. Dominguez, *Boundary Elements in Dynamics*, International Series on Computational Engineering, Computational Mechanics, Southampton; Elsevier Applied Science, London, UK, 1993.

[23] J. Vivoli and P. Filippi, "Eigenfrequencies of thin plates and layer potentials," *Journal of the Acoustical Society of America*, vol. 55, no. 3, pp. 562–567, 1974.

[24] Y. Niwa, S. Kobayashi, and M. Kitahara, "Eigenfrequencies analysis of a plate by the integral equation method," *Theoretical and Applied Mechanics*, vol. 29, pp. 287–307, 1981.

Luiz Carlos Facundo Sanches: Department of Mathematics, Paulista State University,
Al. Rio de Janeiro s/n, 15385-000 Ilha Solteira, SP, Brazil
Email address: luiz@mat.feis.unesp.br

Euclides Mesquita: Department of Computational Mechanics, State University of Campinas,
Rua Mendeleiev s/n, 13083-970 Campinas, SP, Brazil
Email address: euclides@fem.unicamp.br

Renato Pavanello: Department of Computational Mechanics, State University of Campinas,
Rua Mendeleiev s/n, 13083-970 Campinas, SP, Brazil
Email address: pava@fem.unicamp.br

Leandro Palermo Jr.: Department of Structures, State University of Campinas,
Avenida Albert Einstein 951, 13083-970 Campinas, SP, Brazil
Email address: leandro@fec.unicamp.br